DEPARTMENT OF THE AIR FORCE
HEADQUARTERS UNITED STATES AIR FORCE

MAR 8 2001

MEMORANDUM FOR: SAF/PAS
1690 Air Force Pentagon - 5D227
Washington DC 20330-1690

FROM: Francis G. Hinnant, Col, USAF
Associate Director of Acquisition
NPOESS Integrated Program Office
8455 Colesville Rd, Suite 1450
Silver Spring, MD 20910

SUBJECT: Low Wave Infrared, Photovoltaic, FPA Performance for Remote Sensing Applications

Enclosed are the required ten (10) copies of the subject paper. This paper will be presented by Mr. Larry Dawson, Boeing Sensor Products Division, at the Society of Photo-Optical Instrumentation Engineers (SPIE) 15th Annual International Symposium on Aerospace/Defense Sensing, Simulation, and Controls (AEROSENSE) in Orlando, Florida, April 16-20, 2001. Your review is requested by 30 Mar 01.

The program office has reviewed the information and found it appropriate for public disclosure without change. The scientific information contained in this document is considered exempt from United States export control laws under International Traffic in Arms Regulations (ITAR) provision 125.4.b(3)

Point of contact on this matter is Maj Elisa Kang, NPOESS IPO/ADA at 301-427-2084 (Ext. 142).

cc: ADA (E. Kang)

Attachment: Presentation—10 copies

LWIR, Photovoltaic, $Hg_{1-x}Cd_xTe$, FPA Performance, for Remote Sensing Applications

L.C. Dawson, A.I. D'Souza, C. J. Rau, S. Marsh, J.S. Stevens, M.M. Salcido, D.J. Chiaverini, F.W. Mahoney, D.E. Moleneaux, A.A. Bojorquez, C. Staller, C. Yoneyama
Boeing Sensor Products, 3370 Miraloma Avenue, Anaheim, CA 92803

P.S. Wijewarnasuriya, W.V. McLevige
Rockwell Science Center, 1049 Camino Dos Rios, Thousand Oaks, CA 91360

J. Ehlert, J. Jandik, M. Gangl, J. Derr, F. Moore
ITT Aerospace/Communications Division, Ft. Wayne, IN, 46801

Abstract

Focal plane arrays (FPA's), used for remote sensing applications, are required to operate at high temperatures and are subject to high terrestrial background fluxes. Typical remote sensing applications like cloud/weather imagery, sea-surface temperature measurements, ocean color characterization, and land-surface vegetation indices also require FPA's that operate from the visible through the LWIR portion of the spectrum. This combination of harsh requirements have driven the design of a unique LWIR FPA, that operates at 80K under 300K background conditions, with an operating spectral range from 11.5μm to 12.5μm, and a spectral cutoff of 13.5μm.

The FPA consists of 2 side by side arrays of 1x60 HgCdTe, (grown by molecular beam epitaxy) photovoltaic, detector arrays bump bonded to a custom CMOS Si readout. The 2 arrays are completely independent, and can be operated as such. The readout unit cell uses two, current-mode, analog building blocks; a Current Conveyor (CC1)[1] and a dynamic current mirror[2]. The CC1 has input impedance below 300 Ohms and an injection efficiency that is independent of the detector characteristics. This combination extracts high performance and excellent sensitivity from detectors whose average RoA values are approximately 1.7 Ohm-cm^2 at T=80K. The dynamic current mirror is used to subtract high background photocurrent while preserving excellent dynamic range. In addition to the performance enhancing readout, the detectors are manufactured with integral microlenses and operated in reverse bias to take advantage of their increased dynamic impedance. The dark currents associated with reverse bias operation are subtracted along with the background photocurrents by the dynamic current mirror.

The expected and measured LWIR FPA performance will be presented. Measurements were performed on an LWIR FPA. Expected and measured FPA results are shown in the table below. The expected data are calculated from FPA models and compared to the measured values.

	PEAK DSTAR (Jones)	AVERAGE DSTAR (JONES)	MINIMUM RMS NOISE (Volts)	AVERAGE RMS NOISE (Volts)	RESPONSE (Volts)
CALCULATED	3.1E+11		961μV		1.8
MEASURED	>3.0E+11	1.88E+11	1mV	6.2mV	1.4

Table 1: Summary Results Table

1.0 INTRODUCTION

This paper describes the modeled and measured hybrid, LWIR, FPA performance. The FPA was designed for typical remote sensing applications.

2.0 DETECTOR TECHNOLOGY

The diode technology used to implement this focal plane array (FPA) is long wave infrared (LWIR), P on N, photovoltaic, Mercury Cadmium Telluride (HgCdTe), grown by molecular beam epitaxy (MBE) on CdZnTe substrates. The diodes have a spectral cutoff wavelength of λc=13.5μm, and have average Roa products of 1.7 Ω-cm^2 when operated at T=80K. The diodes are formed in two side-by-side linear arrays of 60 diodes each. Each diode has physical dimensions of 250μm in the long direction and 72.1μm in the narrow direction, for a total area of 1.80E-4 cm^2 (See Figure 3). Integral microlenses are produced on each diode to reduce the active area of the diode and thereby increase diode yield. The dimensions of the active area of each diode are 55μm x 40μm, for a total area of 2.20E-5 cm^2. Table 2 is a compilation of relevant detector parameters.

T (K)	80
RoA (Ω-cm^2)	1.7
Cd (Farads)	1.08E-12
QE	.74
Detector Bias	-70mV
RdA (Ω-cm^2)	170
Idark (-70mV) Amps	97.5nA
Phi Background (Ph/cm^2-s)	1.93E+15
Phi Max (Ph/cm^2-s)	2.80E+15
Microlens Area (cm^2)	1.80E-4
Active Area (cm^2)	2.20E-5

Table 2: Measured Detector Characteristics

3.0 AMPLIFIER ARCHITECTURE

The LWIR diodes have an average zero bias source resistance of 77k Ω. This low source resistance makes the LWIR diodes extremely difficult to interface to conventional direct injection (DI) and buffered direct injection (BDI) circuits. Both the DI and BDI suffer from low injection efficiency and lack of detector bias control. To overcome the Shortcomings of the conventional architectures, an amplifier was designed with increased injection efficiency and reduced input impedance. The amplifier provides detector bias control. The amplifier has provisions for removing DC offsets from diode dark and background currents and suppresses low frequency detector noise.

Each detector amplifier unit cell consists of a current conveyor (CC1) followed by a dynamic current mirror and integration capacitor, the schematic is shown in Figure 1.

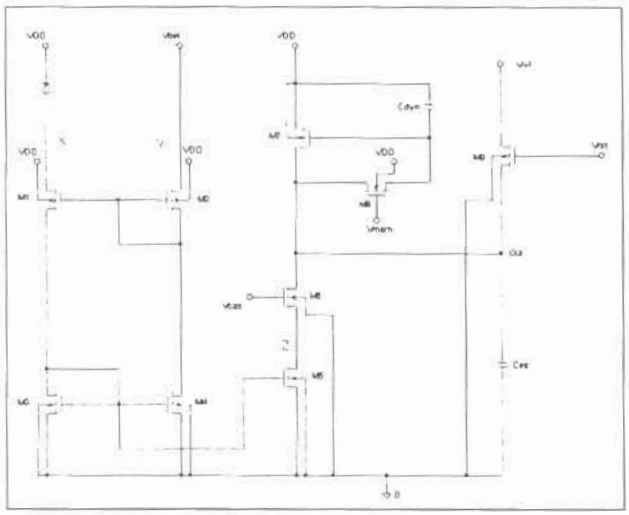

Figure 1: Unit Cell Amplifier Architecture (CC1)

The unit cell is followed by a sample and hold buffer amplifier, sample and hold, multiplexer amplifier, multiplexer and output buffer, a complete block diagram is shown in Figure 2.

The CC1 presents less than 300 Ohms input impedance to the diode, with an injection efficiency that is independent of the diode characteristics. Careful matching of the transistors M1-M5 can give an injection efficiency of 1^3. The CC1 also provides accurate bias control for the diode. The dynamic current mirror restores dynamic range by subtracting off DC current components. The dynamic current mirror also reduces any low frequency detector noise components. The readout was fabricated at AMI using their standard .6μm CMOS process. The layout of the complete IC is shown in Figure 3.

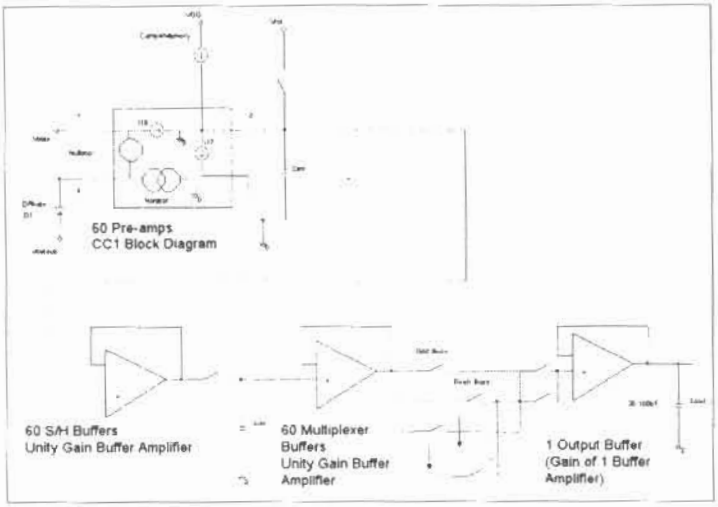

Figure 2: Single Analog Channel Block Diagram

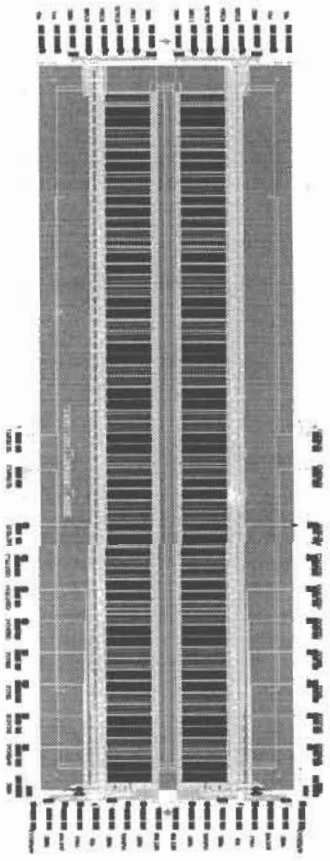

Figure 3: Layout of Detector Amplifier IC

5.0 HYBRID SIMULATION AND MEASURED RESULTS

The hybrid characteristics are compiled in Table 3. The schematic used for simulation and the simulation results are shown in Figures 1 and 4

Tint (sec)	47.76µs
Cint (Farads)	1.54pF
Vswing (Volts)	1.8 Volts
Full Well Capacity	19.3E+6 electrons
Snapshot S/H	Frame time equal Tint (95% duty cycle)
Cal Time	500µs
Interval between Cal	3s

Table 3: Amplifier Characteristics

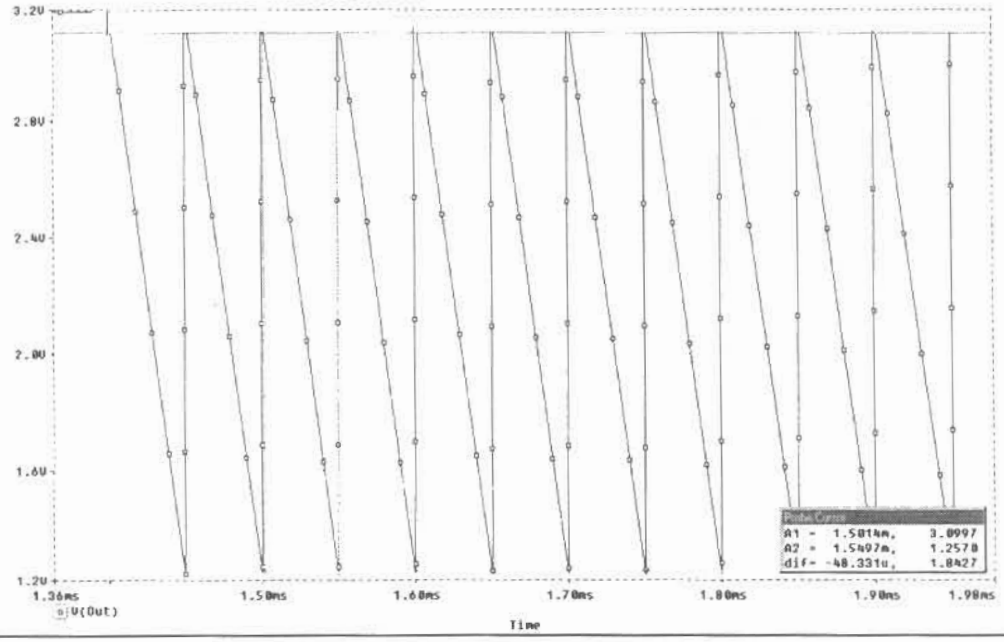

Figure 4: Simulation Results of Signal Integration

It was discovered via flux measurements on the Microlenses that they only transmit 28% of the incident light. All of the fluxes quoted in this text are adjusted for this reduction. The calculated hybrid performance characteristics are shown in Table 4. The measured amplifier noise floor and FPA total RMS noise are shown in Figures 5 and 6. The calculated value of total RMS noise, 960.55µV, compares very well with the minimum measured value of 1mV as shown in Figure 6. 36% of the pixels have total RMS noise less than or equal to 1E-3 Volts. The calculated value of peak Dstar, 3.13E+11 compares very well with the peak measured value of 3.9E11, as shown on the Dstar plot in Figure

7. 29% of the pixels have Dstars above 3.0E+11 and 55% of the pixels have Dstars above 2.0E+11. An NEI plot is shown in Figure 8. The minimum array NEI is 1.23E+12, with an array average NEI of 1.95E+13. Superimposed Oscilloscope plots of response are shown in Figure 9. The background level shown in the figure corresponds to a flux of 1.93E+15 photons/cm^2-s. The 2 other curves shown in Figure 9 correspond to fluxes of 2.15E+15 and 3.47E+15 Respectively. A measured response linearity plot is shown in Figure 10. The response is linear but quite non-uniform. No uniformity correction was applied to any of the Hybrid measurements.

Readout Thermal Noise	335.55μV
Readout 1/f Noise	53.33μV
Readout Switch Noise	29.94μV
Total Amp Noise	341.1μV
Detector Dark Shot Noise	535.89μV
Photon Shot Noise	431.93μV
Detector 1/f Noise	559.2μV
Total Detector Noise	886.82μV
Total Noise	960.55μV
Peak Dstar	3.13E+11 Jones

Table 4: Calculated Performance Characteristics

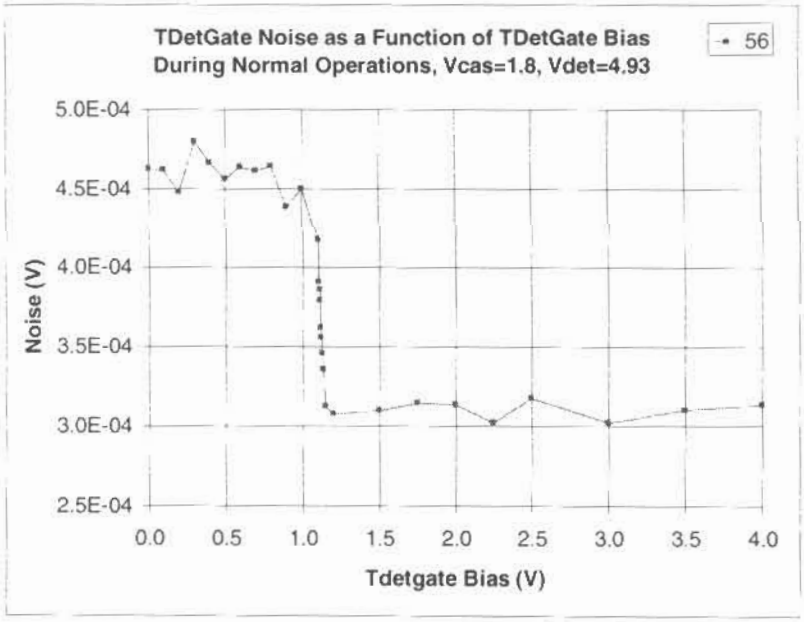

Figure 4: Measured Amplifier Noise Floor

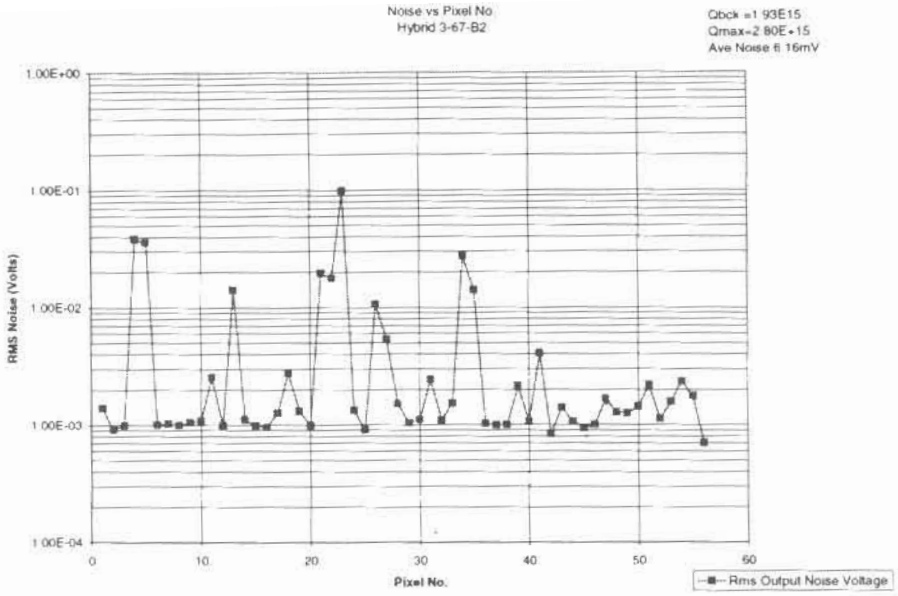

Figure 6: Measured Total RMS Noise for FPA

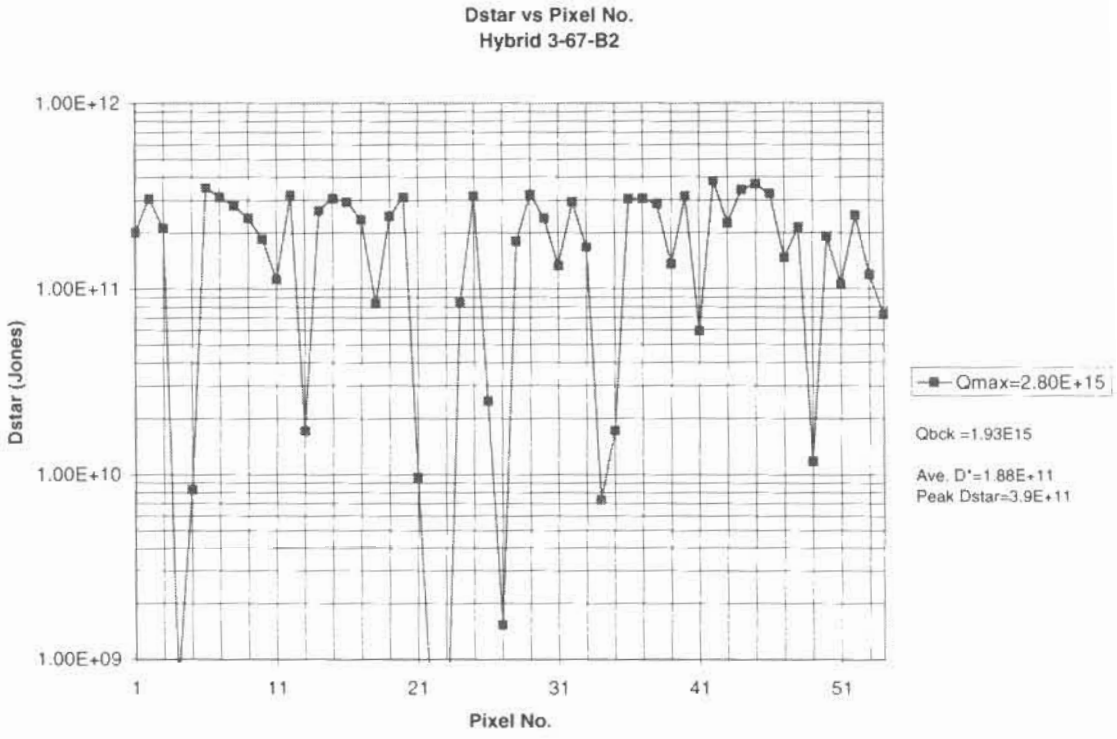

Figure 7: Measured Dstar Skyline Plot for FPA

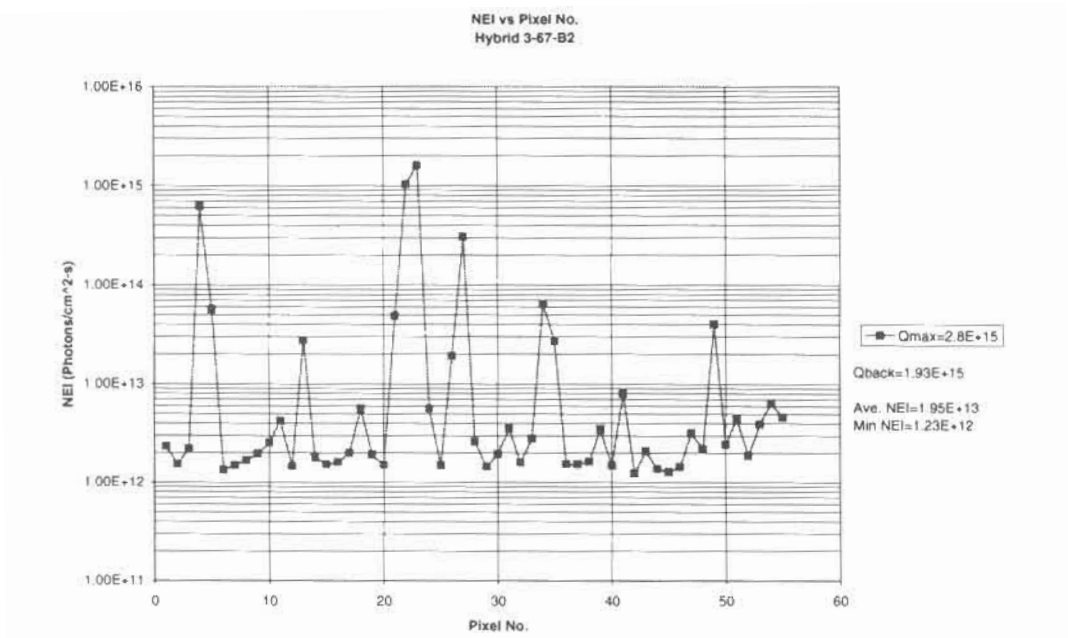

Figure 8: NEI vs. Pixel Number

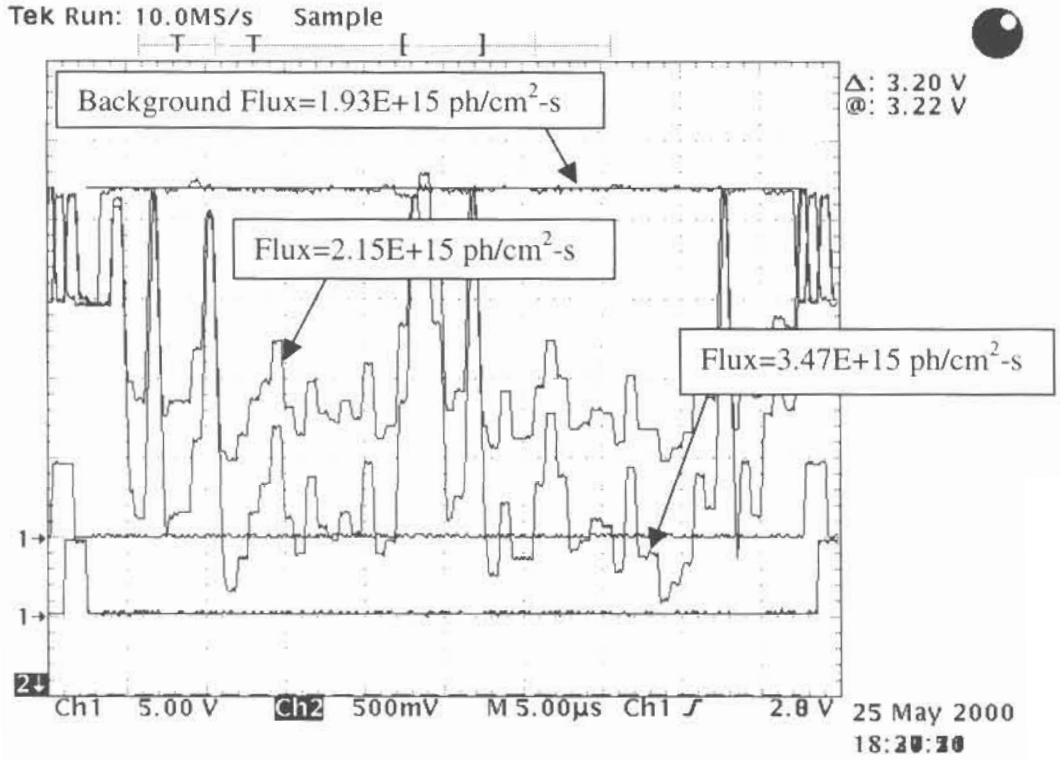

Figure 9: Oscilloscope Trace of Array Response

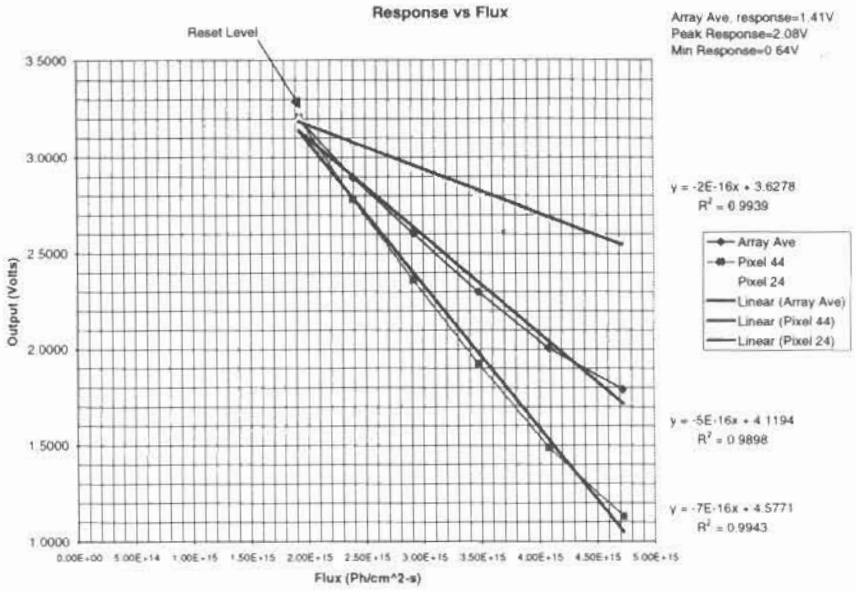

Figure 10: Measured Response

6.0 SUMMARY

A LWIR hybrid FPA was designed and manufactured for use in remote sensing applications. Simulated and measured results were compared.

REFERENCES

1. C. Toumazou, F.J. Lidgey and D.G. Haigh, "Analogue IC Design: the Current Mode Approach", Peter Peregrinus Ltd. On Behalf of the Institution of Electrical Engineers, pp. 94-99

2. C. Toumazou, F.J. Lidgey and D.G. Haigh, "Analogue IC Design: the Current Mode Approach", Peter Peregrinus Ltd. On Behalf of the Institution of Electrical Engineers, pp. 297-325

3. Nanyoung Yoon, Byunghyuck Kim, Hee Chul Lee, Hyungcheol Shin and Choong-Ki Kim, "A New Unit Cell of Current Mirroring Direct Injection Circuit for Focal Plane Arrays", SPIE, Vol. 3061, pp 93-101

FORM CD-15 LF
(REV. 10-93)
DAO 214-2

U.S. DEPARTMENT OF COMMERCE

DATE 7 Mar 01

TRANSMIT/ROUTE SLIP

NAME	BUILDING, ROOM OR REFERENCE NO.	TAKE ACTION BELOW	INITIALS AND DATE
Frank DeLuccia	via e-mail		6 Mar 01
JR Svenson	via e-mail		6 Mar 01
Carol Welsch		(copy)	8 Mar 01 (CW)
Jeff Dedrick	via phone & e-mail		7 Mar 01
Elisa Kang			7 Mar 01
Col Hunnant		1	7 Mar 01

ACTION ITEMS

1. APPROVAL/SIGNATURE
2. CLEARANCE/INITIALS
3. RECOMMENDATION OR COMMENT
4. RETURN WITH MORE DETAILS
5. INVESTIGATE AND REPORT
6. NOTE AND SEE ME
7. NOTE AND RETURN
8. NOTE AND FILE
9. YOUR INFORMATION
10. PER OUR CONVERSATION
11. AS REQUESTED
12. NECESSARY ACTION
13. CIRCULATE AMONG STAFF
14. ANSWER DIRECTLY
15. PREPARE REPLY FOR SIGNATURE OF: _____

COMMENTS

Recommend approving release of Paper (redacted) pending final decision by SAF/PA. Rescind if disapproved - low risk.

☐ Continued on reverse

FROM (Name)	BUILDING, ROOM OR REFERENCE NO.	CODE AND EXTENSION
Elisa		142

NPOESS/ NRA
Maj Kang

LWIR, Photovoltaic, $Hg_{1-x}Cd_xTe$, FPA Performance, for Remote Sensing Applications

L.C. Dawson, A.I. D'Souza, C. J. Rau, S. Marsh, J.S. Stevens, M.M. Salcido, D.J. Chiaverini, F.W. Mahoney, D.E. Moleneaux, A.A. Bojorquez, C. Staller, C. Yoneyama
Boeing Sensor Products, 3370 Miraloma Avenue, Anaheim, CA 92803

P.S. Wijewarnasuriya, W.V. McLevige
Rockwell Science Center, 1049 Camino Dos Rios, Thousand Oaks, CA 91360

J. Ehlert, J. Jandik, M. Gangl, J. Derr, F. Moore
ITT Aerospace/Communications Division, Ft. Wayne, IN, 46801

Abstract

Focal plane arrays (FPA's), used for remote sensing applications, are required to operate at high temperatures and are subject to high terrestrial background fluxes. Typical remote sensing applications like cloud/weather imagery, sea-surface temperature measurements, ocean color characterization, and land-surface vegetation indices also require FPA's that operate from the visible through the LWIR portion of the spectrum. This combination of harsh requirements have driven the design of a unique LWIR FPA, that operates at 80K under 300K background conditions, with an operating spectral range from 11.5μm to 12.5μm, and a spectral cutoff of 13.5μm.

The FPA consists of 2 side by side arrays of 1x60 HgCdTe, (grown by molecular beam epitaxy) photovoltaic, detector arrays bump bonded to a custom CMOS Si readout. The 2 arrays are completely independent, and can be operated as such. The readout unit cell uses two, current-mode, analog building blocks; a Current Conveyor (CC1)[1] and a dynamic current mirror[2]. The CC1 has input impedance below 300 Ohms and an injection efficiency that is independent of the detector characteristics. This combination extracts high performance and excellent sensitivity from detectors whose average RoA values are approximately 1.7 Ohm-cm^2 at T=80K. The dynamic current mirror is used to subtract high background photocurrent while preserving excellent dynamic range. In addition to the performance enhancing readout, the detectors are manufactured with integral microlenses and operated in reverse bias to take advantage of their increased dynamic impedance. The dark currents associated with reverse bias operation are subtracted along with the background photocurrents by the dynamic current mirror.

The expected and measured LWIR FPA performance will be presented. Measurements were performed on an LWIR FPA. Expected and measured FPA results are shown in the table below. The expected data are calculated from FPA models and compared to the measured values.

	PEAK DSTAR (Jones)	AVERAGE DSTAR (JONES)	MINIMUM RMS NOISE (Volts)	AVERAGE RMS NOISE (Volts)	RESPONSE (Volts)
CALCULATED	3.1E+11		961μV		1.8
MEASURED	>3.0E+11	1.88E+11	1mV	6.2mV	1.4

Table 1: Summary Results Table

1.0 INTRODUCTION

This paper describes the modeled and measured hybrid, LWIR, FPA performance. The FPA was designed for typical remote sensing applications.

2.0 DETECTOR TECHNOLOGY

The diode technology used to implement this focal plane array (FPA) is long wave infrared (LWIR), P on N, photovoltaic, Mercury Cadmium Telluride (HgCdTe), grown by molecular beam epitaxy (MBE) on CdZnTe substrates. The diodes have a spectral cutoff wavelength of λc=13.5μm, and have average Roa products of 1.7 Ω-cm^2 when operated at T=80K. The diodes are formed in two side-by-side linear arrays of 60 diodes each. Each diode has physical dimensions of 250μm in the long direction and 72.1μm in the narrow direction, for a total area of 1.80E-4 cm^2 (See Figure 3). Integral microlenses are produced on each diode to reduce the active area of the diode and thereby increase diode yield. The dimensions of the active area of each diode are 55μm x 40μm, for a total area of 2.20E-5 cm^2. Table 2 is a compilation of relevant detector parameters.

T (K)	80
RoA (Ω-cm^2)	1.7
Cd (Farads)	1.08E-12
QE	.74
Detector Bias	-70mV
RdA (Ω-cm^2)	170
Idark (-70mV) Amps	97.5nA
Phi Background (Ph/cm^2-s)	1.93E+15
Phi Max (Ph/cm^2-s)	2.80E+15
Microlens Area (cm^2)	1.80E-4
Active Area (cm^2)	2.20E-5

Table 2: Measured Detector Characteristics

AS AMENDED
per
DTEA

3.0 AMPLIFIER ARCHITECTURE

The LWIR diodes have an average zero bias source resistance of 77k Ω. This low source resistance makes the LWIR diodes extremely difficult to interface to conventional direct injection (DI) and buffered direct injection (BDI) circuits. Both the DI and BDI suffer from low injection efficiency and lack of detector bias control. To overcome the Shortcomings of the conventional architectures, an amplifier was designed with increased injection efficiency and reduced input impedance. The amplifier provides detector bias control. The amplifier has provisions for removing DC offsets from diode dark and background currents and suppresses low frequency detector noise.

Each detector amplifier unit cell consists of a current conveyor (CC1) followed by a dynamic current mirror and integration capacitor, the schematic is shown in Figure 1.

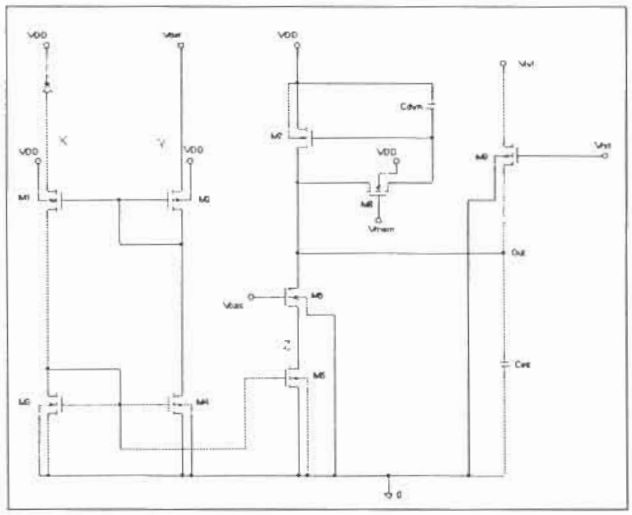

Figure 1: Unit Cell Amplifier Architecture (CC1)

AS AMENDED
per OTRA

The unit cell is followed by a sample and hold buffer amplifier, sample and hold, multiplexer amplifier, multiplexer and output buffer, a complete block diagram is shown in Figure 2.

The CC1 presents less than 300 Ohms input impedance to the diode, with an injection efficiency that is independent of the diode characteristics. Careful matching of the transistors M1-M5 can give an injection efficiency of 1^3. The CC1 also provides accurate bias control for the diode. The dynamic current mirror restores dynamic range by subtracting off DC current components. The dynamic current mirror also reduces any low frequency detector noise components. The readout was fabricated at AMI using their standard .6μm CMOS process. The layout of the complete IC is shown in Figure 3.

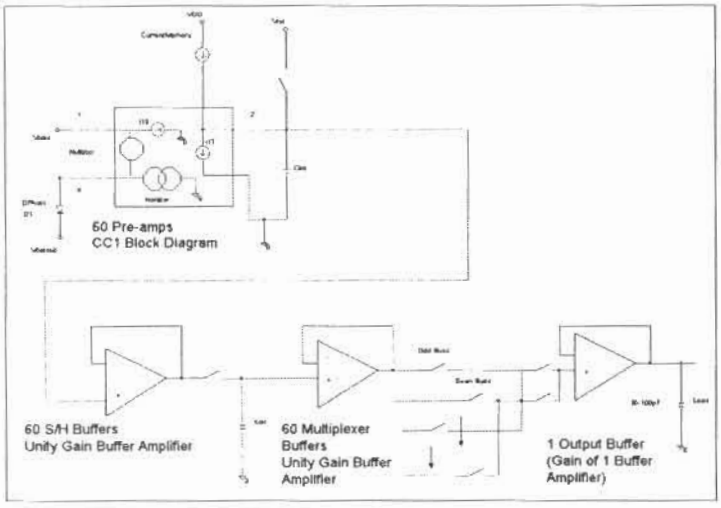

Figure 2: Single Analog Channel Block Diagram

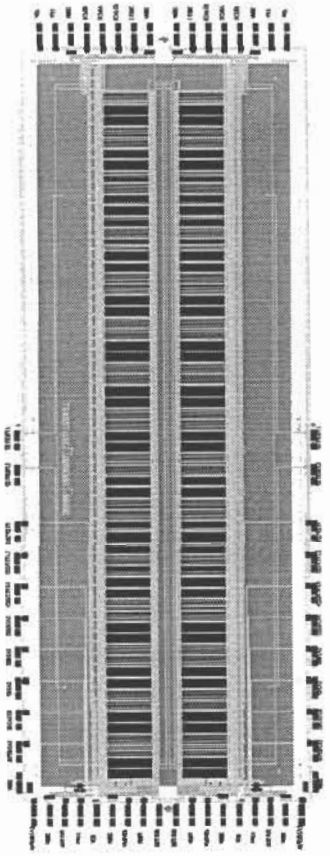

Figure 3: Layout of Detector Amplifier IC

5.0 HYBRID SIMULATION AND MEASURED RESULTS

The hybrid characteristics are compiled in Table 3. The schematic used for simulation and the simulation results are shown in Figures 1 and 4

AS AMENDED per DTRA

Tint (sec)	47.76μs
Cint (Farads)	1.54pF
Vswing (Volts)	1.8 Volts
Full Well Capacity	19.3E+6 electrons
Snapshot S/H	Frame time equal Tint (95% duty cycle)
Cal Time	500μs
Interval between Cal	3s

Table 3: Amplifier Characteristics

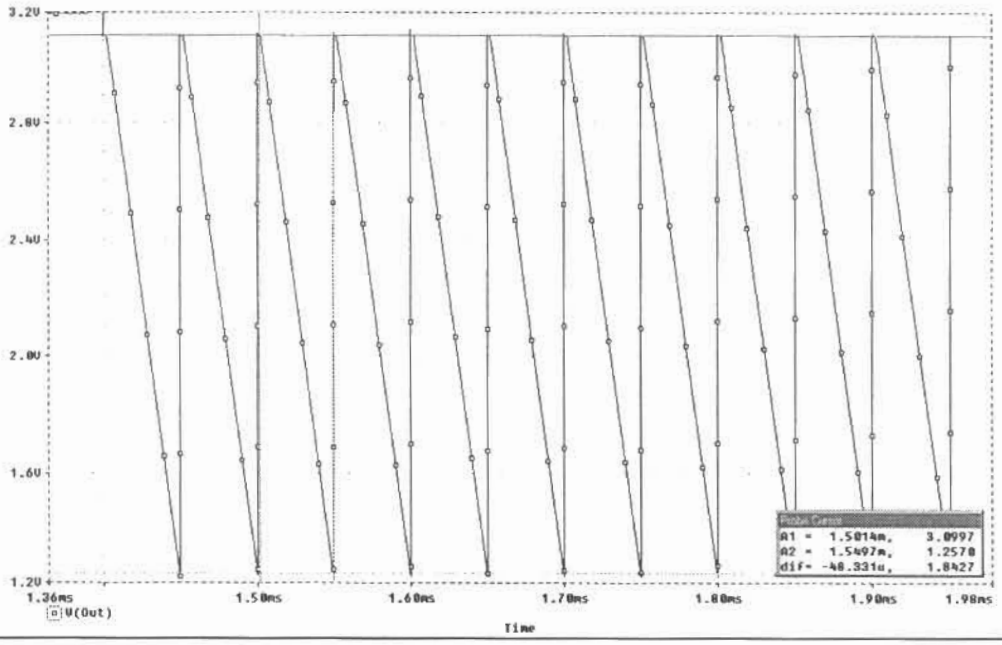

Figure 4: Simulation Results of Signal Integration

It was discovered via flux measurements on the Microlenses that they only transmit 28% of the incident light. All of the fluxes quoted in this text are adjusted for this reduction. The calculated hybrid performance characteristics are shown in Table 4. The measured amplifier noise floor and FPA total RMS noise are shown in Figures 5 and 6. The calculated value of total RMS noise, 960.55μV, compares very well with the minimum measured value of 1mV as shown in Figure 6. 36% of the pixels have total RMS noise less than or equal to 1E-3 Volts. The calculated value of peak Dstar, 3.13E+11 compares very well with the peak measured value of 3.9E11, as shown on the Dstar plot in Figure

7. 29% of the pixels have Dstars above 3.0E+11 and 55% of the pixels have Dstars above 2.0E+11. An NEI plot is shown in Figure 8. The minimum array NEI is 1.23E+12, with an array average NEI of 1.95E+13. Superimposed Oscilloscope plots of response are shown in Figure 9. The background level shown in the figure corresponds to a flux of 1.93E+15 photons/cm^2-s. The 2 other curves shown in Figure 9 correspond to fluxes of 2.15E+15 and 3.47E+15 Respectively. A measured response linearity plot is shown in Figure 10. The response is linear but quite non-uniform. No uniformity correction was applied to any of the Hybrid measurements.

AS AMENDED
Per OTRA

Readout Thermal Noise	335.55μV
Readout 1/f Noise	53.33μV
Readout Switch Noise	29.94μV
Total Amp Noise	341.1μV
Detector Dark Shot Noise	535.89μV
Photon Shot Noise	431.93μV
Detector 1/f Noise	559.2μV
Total Detector Noise	886.82μV
Total Noise	960.55μV
Peak Dstar	3.13E+11 Jones

Table 4: Calculated Performance Characteristics

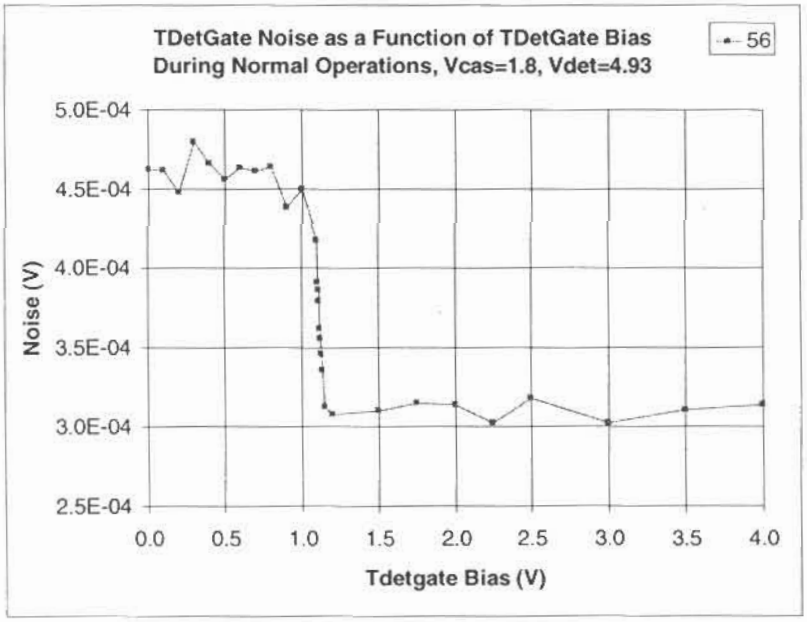

Figure 4: Measured Amplifier Noise Floor

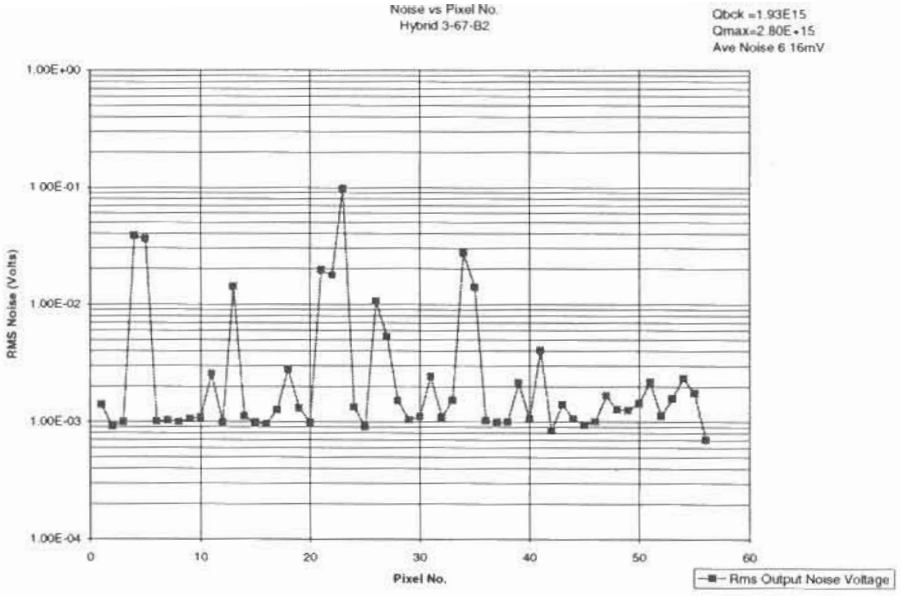

Figure 6: Measured Total RMS Noise for FPA

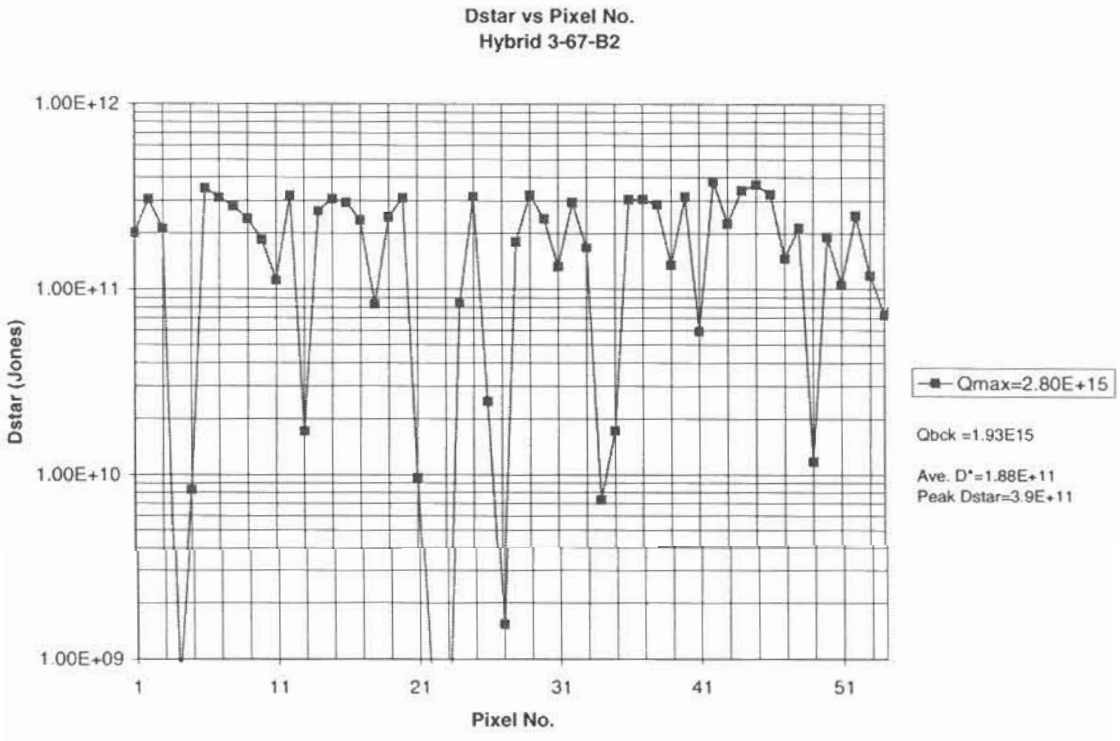

Figure 7: Measured Dstar Skyline Plot for FPA

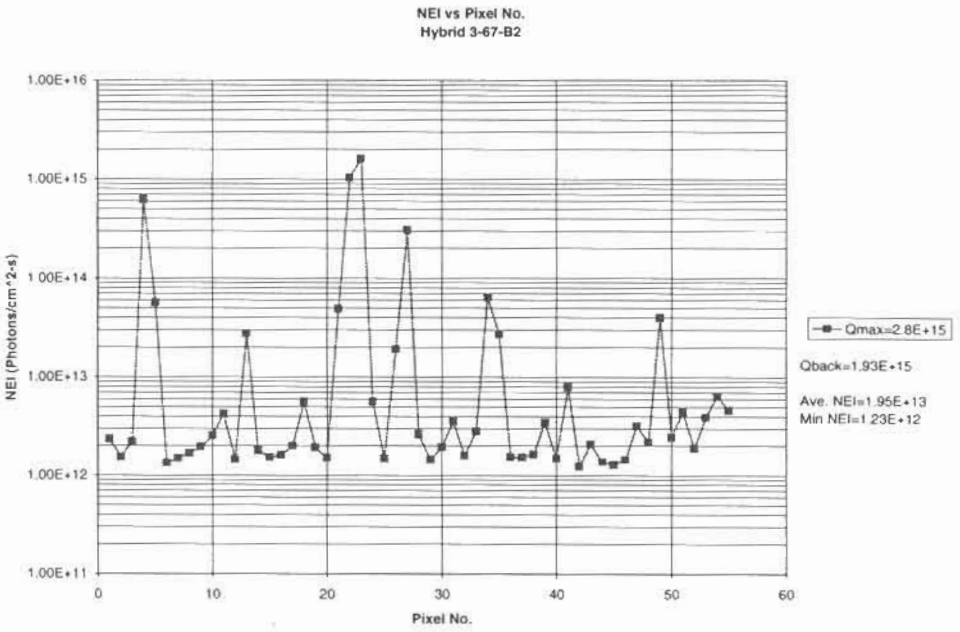

Figure 8: NEI vs. Pixel Number

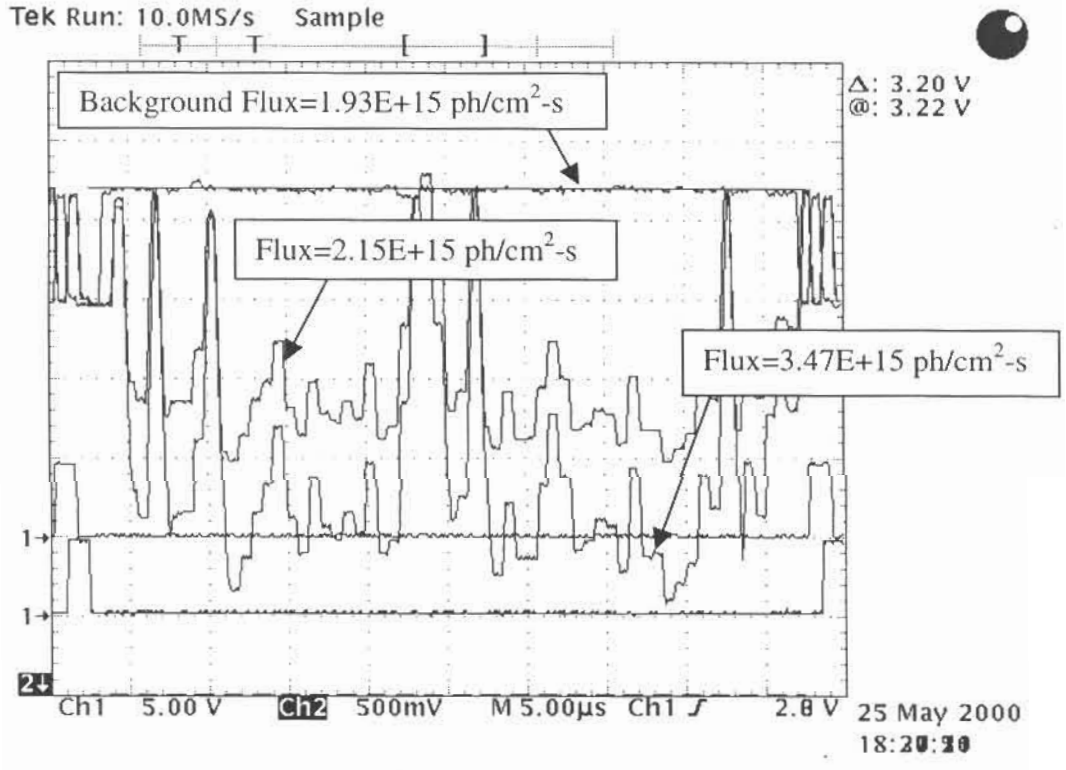

Figure 9: Oscilloscope Trace of Array Response

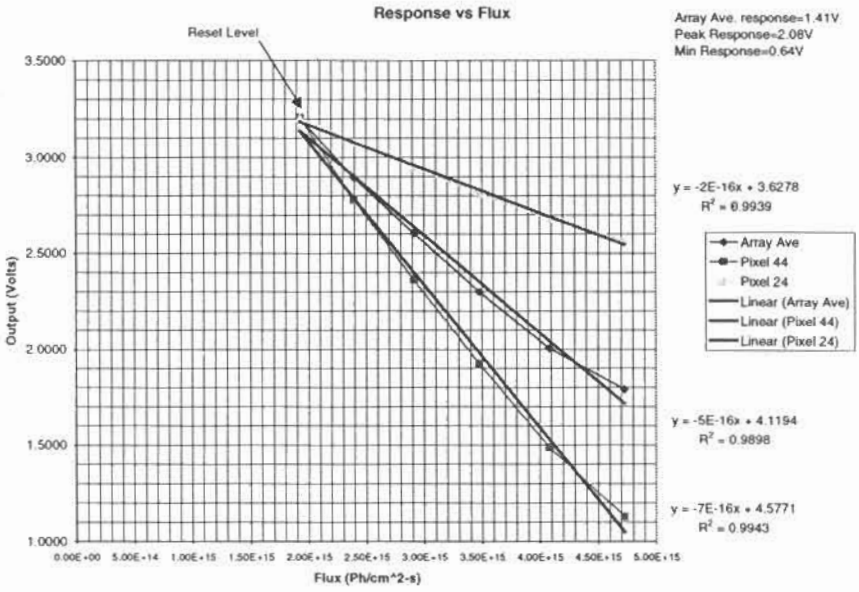

Figure 10: Measured Response

6.0 SUMMARY

A LWIR hybrid FPA was designed and manufactured for use in remote sensing applications. Simulated and measured results were compared.

REFERENCES

1. C. Toumazou, F.J. Lidgey and D.G. Haigh, "Analogue IC Design: the Current Mode Approach", Peter Peregrinus Ltd. On Behalf of the Institution of Electrical Engineers, pp. 94-99

2. C. Toumazou, F.J. Lidgey and D.G. Haigh, "Analogue IC Design: the Current Mode Approach", Peter Peregrinus Ltd. On Behalf of the Institution of Electrical Engineers, pp. 297-325

3. Nanyoung Yoon, Byunghyuck Kim, Hee Chul Lee, Hyungcheol Shin and Choong-Ki Kim, "A New Unit Cell of Current Mirroring Direct Injection Circuit for Focal Plane Arrays", SPIE, Vol. 3061, pp 93-101